Radiology

Evaluation of a Flexible 12-Channel Screen-printed Pediatric MRI Coil

Simone Angela Winkler, PhD • Joseph Corea, PhD • Balthazar Lechêne, PhD • Kendall O'Brien, BA • John Ross Bonanni, MD • Akshay Chaudhari, PhD • Marcus Alley, PhD • Valentina Taviani, PhD • Thomas Grafendorfer, PhD • Fraser Robb, PhD • Greig Scott, PhD • John Pauly, PhD • Michael Lustig, PhD • Ana Claudia Arias, PhD • Shreyas Vasanawala, MD, PhD

From the Department of Radiology, Stanford University, 300 Pasteur Dr, Stanford, CA 94305 (S.A.W., A.C., M.A., S.V.); Department of Electrical Engineering and Computer Sciences, University of California, Berkeley, Calif (J.C., B.L., M.L., A.C.A.); Lucile Packard Children's Hospital at Stanford, Stanford, Calif (K.O., J.R.B.); GE Healthcare, Menlo Park, Calif (V.T.); GE Healthcare, Aurora, Ohio (T.G., F.R.); and Department of Electrical Engineering, Stanford University, Stanford, Calif (G.S., J.P.). Received August 10, 2018; revision requested September 4; revision received January 7, 2019; accepted January 10. **Address correspondence to** S.A.W. (e-mail: *simone.winkler@stanford.edu*).

Supported by GE Healthcare, the National Institute of Biomedical Imaging and Bioengineering (K99 EB24341, R01 EB009690, R01 EB019241, R21 EB015628), and the Bakar Foundation.

Conflicts of interest are listed at the end of this article.

See also the editorial by Lamb in this issue.

Radiology 2019; 291:180–185 • https://doi.org/10.1148/radiol.2019181883 • Content codes: PD MR

Background: Screen-printed MRI coil technology may reduce the need for bulky and heavy housing of coil electronics and may provide a better fit to patient anatomy to improve coil performance.

Purpose: To assess the performance and caregiver and clinician acceptance of a pediatric-sized screen-printed flexible MRI coil array as compared with conventional coil technology.

Materials and Methods: A pediatric-sized 12-channel coil array was designed by using a screen-printing process. Element coupling and phantom signal-to-noise ratio (SNR) were assessed. Subjects were scanned by using the pediatric printed array between September and November 2017; results were compared with three age- and sex-matched historical control subjects by using a commercial 32-channel cardiac array at 3 T. Caregiver acceptance was assessed by asking nurses, technologists, anesthesiologists, and subjects or parents to rate their coil preference. Diagnostic quality of the images was evaluated by using a Likert scale (5 = high image quality, 1 = nondiagnostic). Image SNR was evaluated and compared.

Results: Twenty study participants were evaluated with the screen-printed coil (age range, 2 days to 12 years; 11 male and nine female subjects). Loaded pediatric phantom testing yielded similar noise covariance matrices and only slightly degraded SNR for the printed coil as compared with the commercial coil. The caregiver acceptance survey yielded a mean score of 4.1 ± 0.6 (scale: 1, preferred the commercial coil; 5, preferred the printed coil). Diagnostic quality score was 4.5 ± 0.6. Mean image SNR was 54 ± 49 (paraspinal muscle), 78 ± 51 (abdominal wall muscle), and 59 ± 35 (psoas) for the printed coil, as compared with 64 ± 55, 65 ± 48, and 57 ± 43, respectively, for the commercial coil; these SNR differences were not statistically significant ($P = .26$).

Conclusion: A flexible screen-printed pediatric MRI receive coil yields adequate signal-to-noise ratio in phantoms and pediatric study participants, with similar image quality but higher preference by subjects and their caregivers when compared with a conventional MRI coil.

© RSNA, 2019

Online supplemental material is available for this article.

Pediatric MRI is often performed with heavy, large, and relatively inflexible coil arrays designed and built for adult MRI. For awake children, these arrays can be intimidating and uncomfortable, thereby restricting the child's breathing. For parents, they contribute to the stress of the examination. For pediatric caregivers, the coils complicate the placement of medical support equipment, such as mechanical ventilation tubes, pulse oximeters, anesthetic lines, respiratory bellows, blood pressure cuffs, electrocardiogram probes, and video goggles. For sedated or anesthetized children, respiratory compromise from heavy coils on the torso requires more invasive respiratory support or bolstering of the coils away from the patient, with a resultant decrease in signal-to-noise ratio (SNR) and reduced parallel imaging acceleration capability. As a result, much work has been aimed at the design of custom-fitted pediatric coils to maintain SNR. Such efforts have included a flexible cardiac array (1), a set of small head coils for pediatric patients (2), and even a novel pneumatically adjustable head coil to maintain a close patient fit (3). In comparison, flexible arrays have also been proposed by Neocoil (Pewaukee, Wis) and ScanMed (Omaha, Neb).

Recently, screen-printed MRI coil technology has been developed to increase SNR due to a more compact fit with respect to the patient. Screen-printed MRI coils allow printing on a flexible substrate (4,5). These coils also have been shown to be printable on fabric, and a 12-channel receive array has been used at 3 T (4–7). In addition to the beneficial SNR increase of large dense MRI coil arrays in general (1,8–14), screen-printed technology (15,16) offers the advantage

This copy is for personal use only. To order printed copies, contact *reprints@rsna.org*

Abbreviations

FOV = field of view, ROI = region of interest, SNR = signal-to-noise ratio

Summary

A screen-printed pediatric MRI coil yielded diagnostic image quality and a signal-to-noise ratio that was comparable to that of a commercial 32-channel adult coil and had greater flexibility and comfort.

Key Points

- A pediatric-sized, 12-channel screen-printed MRI receive coil yielded diagnostic image quality and signal-to-noise ratio comparable to those of a commercial 32-channel adult cardiac array for pediatric patients.
- A pediatric-sized, 12-channel screen-printed MRI receive coil was preferred to a commercial 32-channel adult cardiac array MRI coil by patients, parents, and caregivers due to increased flexibility and comfort.

of eliminating the need for bulky and heavy housing of coil electronics.

In this work, we assessed the use of a 12-channel screen-printed flexible coil array (1–7) for pediatric applications, focusing on feasibility of use in the clinical setting, image quality, and caregiver acceptance. We also compared SNR with the screen-printed coil with that of a conventional coil routinely used for pediatric imaging. We hypothesized that image SNR would be maintained, images of diagnostic quality would be obtained, and patients, parents, and caregivers may prefer screen-printed coils.

Materials and Methods

One author (F.R.) is an employee of GE Healthcare; GE Healthcare also gave financial support for this study. Several other authors (J.C., B.L., V.T., T.G., M.L., and A.C.A.) are affiliated with InkSpace Imaging. Those authors who are not employees of or consultants for InkSpace Imaging or GE Healthcare had control over the inclusion of any data or information that might have presented a conflict of interest for the aforementioned authors.

This study was approved by the institutional review board, and informed consent was obtained. Twenty consecutive pediatric study participants were referred for a 3-T clinical MRI between September 2017 and November 2017 and were recruited for this prospective study in compliance with the Health Insurance Portability and Accountability Act. The exclusion criteria were contraindications to MRI and age greater than 12 years (the 12-channel screen-printed pediatric coil array would have been too small for patients older than 12 years). Study participants were scanned with a 12-channel screen-printed coil by using institutional standard clinical protocols (Table).

Coil Design and Construction

One month of pediatric abdominal and MRI chest scan data were analyzed for patient size to determine appropriate pediatric array size (Fig E1 [online]).

Screen printing is an additive manufacturing process that creates patterns by depositing materials in single layers onto a flat substrate by forcing ink though holes in a patterned mesh called a screen (4).

The 12-channel prototype array was built by screen-printing 15-μm-thick conductive traces (118–09; Creative Materials, Ayer, Mass) onto 76-μm-thick polyether ether ketone substrates (Fig 1, *A*) to make the array thin and flexible.

The conductivity of the ink (DuPont 5064H; DuPont, Wilmington, Del) is 1.84×10^{-5} Ω·cm, as measured with a four-point probe, whereas that of copper is 1.7×10^{-8} Ω·m. The dry ink is composed of silver microflake particles (particle size <9 μm) immersed in a polymer-based binder with a minimal amount of residual solvent.

The array was encapsulated in 76 μm of Teflon, then affixed onto a 200-μm-thick fireproof fabric and sealed in a patterned waterproof fabriclike coating that resembled a blanket to increase patient comfort. The six octagonal 15 × 8 cm elements in the array cover a 27 × 27 cm area in each paddle. The flexible portion of the array contains the conductive loops of the coil, as well as a small matching and spoiling board; the preamplifiers are positioned remotely inside a third-party gateway that interfaces with the imager (Gateway; MR Solutions, Brookfield, Wis) (Fig 1, *A*).

Coil Safety Testing

Prior to scanning any subjects, all prototype coils were tested for patient safety. Each coil element had its blocking circuit characterized to ensure a blocking impedance to coil area greater than 0.75 Ω/cm² during transmission. A power dissipation analysis was performed to ensure that each circuit element was at or below the component manufacturer ratings. The coil was encapsulated with UL94 V0 fire-rated materials. Coils were tested with a modified gradient-echo sequence on a Discovery MR750 3-T imager (GE Healthcare, Waukesha, Wis) that exceeded the maximum radiofrequency power for 45 minutes and were examined with a thermal camera to ensure no portion of the coil exceeded 41°C. Finally, a modified single-shot fast spin-echo sequence that exceeded the maximum peak radiofrequency voltage was used to test for arcing.

Phantom Noise Performance Assessment

To compare array performance, the 12-channel printed pediatric coil was compared with the 32-channel commercial coil. The printed coil was assessed in a tightly wrapped and gently laid configuration on a 32-cm-long, 19-cm-wide, and 9-cm-thick pediatric patient–shaped phantom (Fig 2, *A*) with 3.37 g/L $NiCl_2 \cdot 6 H_20$ and 2.5 g/L NaCl (yielding $\sigma \approx 0.5$ S/m, $\varepsilon_r \approx 70$). Coil sensitivities were estimated by using ESPIRiT (an eigenvalue approach to autocalibrating parallel MRI) (17) and were used to produce SNR maps and noise correlation profiles. A 256 × 256 two-dimensional spin-echo sequence (repetition time msec/echo time msec, 500/20 ; section thickness, 10 mm; section spacing, 10 mm; in-plane field of view [FOV], 20 × 20 cm) was used to assess noise performance for both coils, with the imager radiofrequency transmitter disabled. SNR maps for accelerations in the superior-inferior and right-left directions were established.

Caregiver Acceptance Assessment

For each subject, each caregiver, including the MRI technologist, nurse, and anesthesiologist, was surveyed with a printed question-

Table 1: MRI Pulse Sequences Used in this Study

Abdominal-Pelvic	Cardiac	MR Cholangiopancreatography
Coronal SSFSE	Axial time-resolved volumetric phase contrast	Coronal SSFSE
Coronal volumetric T2 FSE	Axial ultrasort echo-time MR angiography	Axial SSFSE
Axial T2 FSE	Balanced steady-state free precession	Coronal 3D FSE
Axial DW imaging	…	Coronal fat-suppressed 3D SPGR
Coronal fat-suppressed 3D SPGR	…	Axial fat-suppressed 3D SPGR
Axial ultrashort echo time with contrast enhancement	…	…
Axial 3D SPGR with two-point Dixon	…	…

Note.—DW = diffusion-weighted, FSE = fast spin-echo, SPGR = spoiled gradient recall, SSFSE = single-shot fast spin-echo, 3D = three-dimensional.

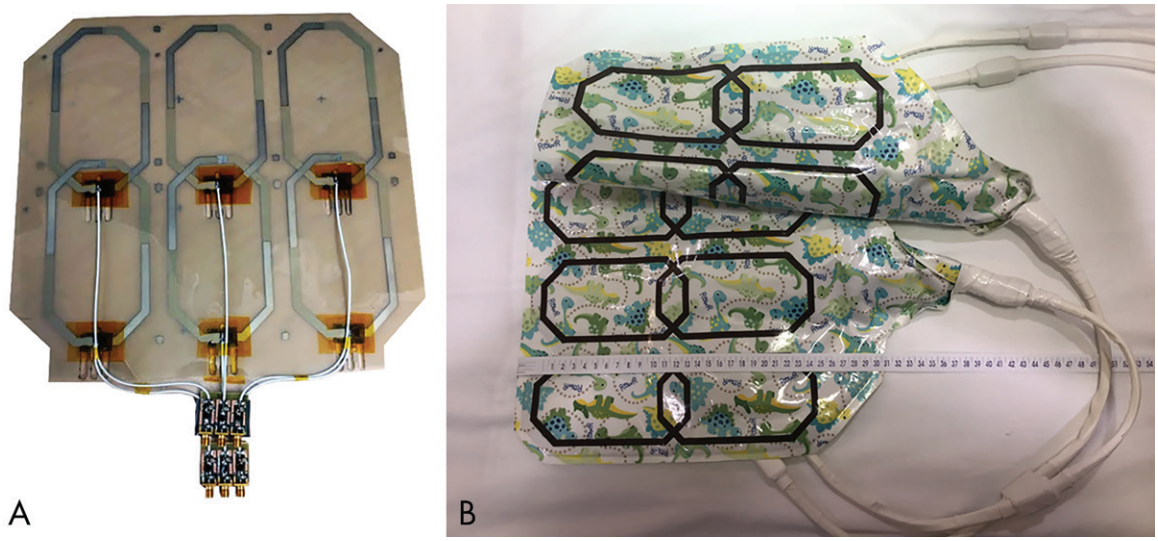

Figure 1: Screen-printed 12-channel coil array for pediatric applications allows for ease of construction, flexibility, lighter weight, and smaller size arrays, offering easy access to monitoring equipment. *A,* Interior coil construction (anterior and posterior components are constructed equally). *B,* Complete array demonstrates flexibility by the anterior component being folded in the longitudinal direction.

naire to assess the level of acceptance of the printed coil. Children who were able to complete the survey did so (five study participants), and parents recorded their feedback whenever children were unable to because of anesthesia or young age. Technologists recorded the *(a)* ease of positioning; *(b)* coil preference for the specific examination, subject, or both; and *(c)* overall coil preference for the examination. Anesthesiologists and nurses were queried on *(a)* choice of airway, *(b)* choice of anesthetic, and *(c)* overall coil preference. Each preference was recorded on a scale from 1 (preferred traditional coil) to 5 (preferred printed coil). Additionally, comments in the form of open-ended feedback were recorded.

Diagnostic Image Quality

A radiologist (S.V., 15 years of experience interpreting MRI studies) classified all studies by using a Likert scale (5, high image quality across all of the anatomy and all of the sequences; 4, good image quality across either all of the anatomy or all of the sequences; 3, good image quality across some of the anatomy and some of the sequences; 2, limited examination; 1, nondiagnostic). A case–control study was performed, with 1:3 matching of cases to control subjects.

In Vivo SNR Evaluation

To compare imaging performance, SNR was evaluated on a respiratory triggered axial T2 image (echo time, 80 msec; no fat saturation; receiver bandwidth, 62.5 Hz). The time needed to acquire 28 sections was approximately 90 seconds, depending on respiratory triggering. To ensure accurate SNR measurements, the sequence did not use acceleration, and all filtering and surface intensity correction were disabled. The SNR evaluation sequence used a baseline FOV of 24.0 × 16.8 cm and a section thickness of 5 mm, with a matrix size of 320 × 224 voxels, resulting in a baseline voxel size of 0.75 × 0.75 × 5 mm. This FOV was applicable to a large portion of study participants. Wherever this FOV was not appropriate, a different voxel size resulted, and we normalized the SNR to the baseline voxel size.

SNR was measured as the ratio of the mean signal value and the background standard deviation, using the same region of interest (ROI) for each case. SNR was compared for examinations that used gadobutrol as the intravenous contrast agent to avoid error from ferumoxytol signal intensity variation and was measured in a non–fat-containing region of the lumbar paraspinal muscles and in abdominal wall muscle tissue, as well as

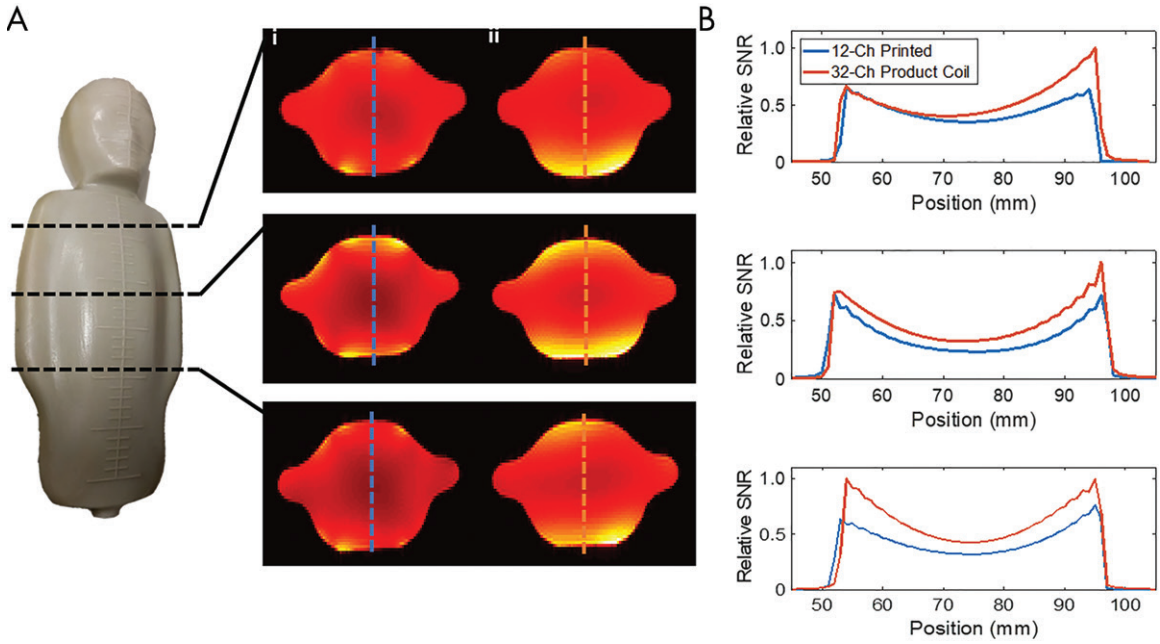

Figure 2: *A,* Pediatric phantom highlights the location of axial signal-to-noise ratio (SNR) maps produced with the 12-channel printed coil *(i)* and the 32-channel printed array *(ii)*. Blue and red dotted lines indicate location of SNR profile highlighted in *B*. *A,* Plots comparing SNR through the phantom for the 12-channel printed coil and the 32-channel coil to that of the screen-printed coil.

in the psoas muscle for assessment of SNR behavior in deeper regions of the body. A case–control study was performed, with 1:3 matching of cases to control subjects.

Statistical Methods

Phantom tests.—The method descried by Kellman and McVeigh (18) was used to calculate SNR values during imaging of the phantom. Noise-only images were acquired immediately after a normal examination and contained 65 536 pixels to estimate the noise.

In vivo SNR methods.—We used the Wilcoxon signed-rank test to evaluate the statistical significance of differences in SNR between the screen-printed coil and the commercial adult coil.

Caregiver survey.—Confidence intervals were calculated for the proportion of scores above three and the proportion of scores above four.

Diagnostic acceptability.—Confidence intervals were calculated for the proportion of scores above three and the proportion of scores above four.

Results

Study Participant Demographics

Subject age ranged from 2 days to 12 years, subject weight ranged from 1.8 to 57.0 kg, and abdominal-pelvic (nine study participants), pancreas or gallbladder (three study participants), cardiac (three study participants), chest (three study participants), and upper extremity (two study participants) imaging was performed. Nine study participants were female, and 11 were male. Ten study participants were scanned with ferumoxytol; nine, with gadobutrol; and one, with no intravenous contrast agent. Fourteen study participants received anesthesia.

Coil Design and Construction

The largest gap in array size suggested that patients aged 0–5 years were not taking advantage of all 32 elements of the array (Fig E1 [online]) (6). We determined that a 27.0 × 26.7 cm array would fit the torso of 0–2-year-old patients and would cover the chest and/or abdomen of 3–5-year-old patients. As a result, the array is designed by using three elements in the left-right direction and two elements in the superior-inferior direction, measuring 15 × 8 cm each, for a total of six elements in both the anterior and posterior portions of the array (Fig 1, *A*). Coils were overlapped lengthwise but not across the body. The anterior portion placed on the patient weighed 360 g, with total outer dimensions of 34 × 30 cm in the superior-inferior direction (Fig 1, *B*), whereas the anterior part of the commercial adult coil weighed 2.9 kg, with superior-interior outer dimensions of 33 × 40 cm.

Coil Safety Testing

All prototype coils passed safety tests, as described in Materials and Methods.

Phantom Noise Performance Assessment

SNR profiles were compared at select locations (Fig 2, *A*). Noise correlations for both coils are shown in Figure E2 (online). The printed coil array showed a mean correlation of 0.09 ± 0.05, with a maximum correlation of 0.21, while

commercial 32-channel imagers had a mean correlation of 0.08 ± 0.04, with a maximum correlation of 0.27.

SNR maps denoting acceleration factors of 1.5 times in the superior-inferior direction and 2.6 times in the right-left direction are shown in Figure E3 (online). Bright areas indicate areas with no SNR loss; darker areas show areas of SNR loss due to acceleration. As is shown, the 12-channel screen-printed coil has a better *g*-factor map because more elements are in the FOV as compared with the poorly fitting 32-channel commercial coil.

Caregiver Acceptance

In the subject and provider survey, we obtained a mean overall score of 4.1 ± 0.6 (Likert scale: 1, preferred traditional coil; 5, preferred screen-printed coil), indicating preference for the screen-printed coil (Table E1 [online]). Technologists, anesthesiologists, nurses, and parents and/or children favored the new screen-printed coil technology in their overall preference rating, with mean scores of 4.2 ± 1.5, 3.6 ± 1.2, 4.2 ± 0.9, and 4.5 ± 1.1, respectively.

Diagnostic Image Quality Assessment

The radiologist rated all 20 cases as diagnostically acceptable, with an average score of 4.5 ± 0.6 (80% confidence interval: 4.3, 4.7), and no repeat examinations with a different coil were required. The confidence level for scores to be 4 or greater was 99.8%. Although this was not part of the prospective evaluation of the printed coil, we retrospectively identified several subjects who had undergone prior imaging of the same body part with the commercial coil. Figure 3 shows three comparisons of images between the commercial coil and the 12-channel screen-printed coil in these subjects. Additional images obtained with the printed coil are shown in Figure E4 (online).

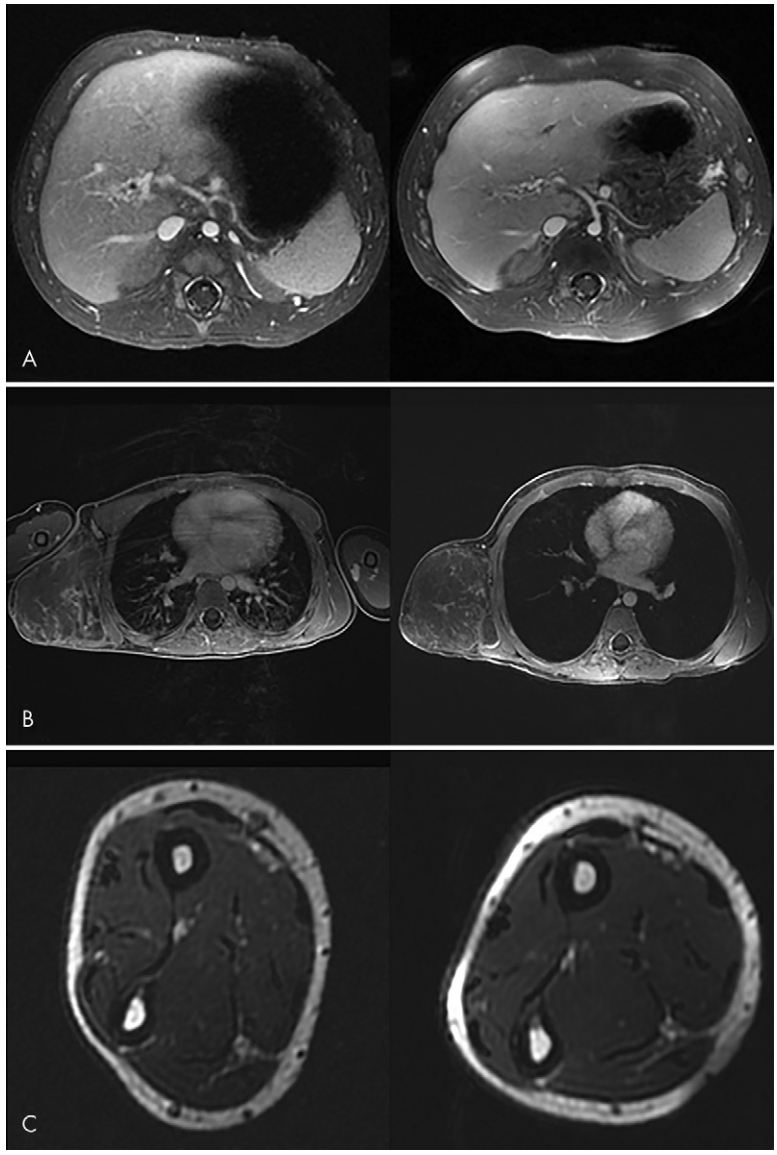

Figure 3: Comparison of clinical MR images obtained with commercial (left) and 12-channel screen-printed (right) coils. *A,* Abdominal image in a 3-month-old subject with cavernous transformation of the portal vein. *B,* Chest image in a 7-year-old subject with a chest wall vascular malformation. *C,* Forearm image in a 12-year-old subject. Good field of view coverage and high signal-to-noise ratio are demonstrated.

In Vivo SNR Evaluation

Mean in vivo normalized SNR was 54 ± 49 in paraspinal muscle, 78 ± 51 in abdominal wall muscle, and 59 ± 35 in the psoas for the printed coil, as compared with 64 ± 55, 65 ± 48, and 57 ± 43, respectively, for the commercial coil. When we used the Wilcoxon signed-rank test, the SNR of the screen-printed coil was not different from the SNR of the commercial adult coil (P = .26).

Discussion

In this study, we described the design, construction, and pilot clinical use of pediatric screen-printed coil technology. We assessed caregiver acceptance of the new coil and studied diagnostic image quality and SNR in comparison with a commonly used commercial adult coil. Our major findings are that caregivers prefer the screen-printed coils and that diagnostic image quality is highly likely to be obtained with a survey score of 4.1 (scale: 1, prefer traditional coil; 3, no preference; 5, prefer printed coil). We also achieved comparable in vivo SNR for the printed coil compared with a commercially available adult MRI coil (P = .26 for comparison of SNR).

Overall, the new technology was very well received. The open-ended feedback focused on the lightweight, soft, and flexible aspects of the coil, as well as the minimization of respiratory compromise form pressure on the chest. Clinical caregivers also noted that children, their parents, or both commented on the increased comfort of the lighter weight coil. Technologists specified the ease of positioning.

Areas noted for improvement by caregivers included potential padding of the cable to prevent discomfort during chest

imaging and stiffening the coil to improve respiratory bellows in a few isolated cases.

All images were rated to exhibit suitable diagnostic image quality, and both independent radiologists agreed on all cases. The pediatric screen-printed coil exhibits a smaller size (coverage of 27 × 27 cm) than the commercial adult coil; therefore, it was used only in children who weighed less than 20 kg.

The noise correlation in a phantom was determined to be similar when using the screen-printed and commercial adult coils, which is concordant with the clinical diagnostic imaging quality assessment. SNR was slightly degraded in phantom measurements for the screen-printed coil array, which was attributed to the larger element size, lower channel count, large separation of preamplifiers from coil elements, and lossier coil material. However, we noted an increase in SNR with the screen-printed coil relative to the conventional coil in vivo, which is likely related to the ease of placing the screen-printed coil in closer proximity to pediatric subjects. We also observed less SNR homogeneity as a result. If more homogeneous SNR is desired, surface coil correction can be used.

A limiting factor in our study was that we did not examine the same subject with both the new screen-printed coil and the conventional 32-channel commercial adult coil, although we were able to show a few selected direct comparisons in Figure 3 for illustrative purposes. Instead, comparison phantom studies were performed. In the limited clinical setting, we were only able to evaluate axial images for in vivo SNR.

We also used the same coil size for all subjects, who ranged in age from 2 days to 12 years. We used an adult-sized commercial coil for control subjects of all ages.

In conclusion, we demonstrated that a pediatric flexible 12-channel screen-printed MRI receive coil yields diagnostic image quality and is likely to be preferred to a traditional coil by subjects, parents, and caregivers. The screen-printed MRI receive coil had a high signal-to-noise ratio that was comparable to that of a commercially available surface coil.

Acknowledgments: The authors thank Jon Tamir, PhD, at University of California, Berkeley, as well as the Lucile Packard Children's Hospital staff for their valuable time and support.

Author contributions: Guarantor of integrity of entire study, S.A.W.; study concepts/study design or data acquisition or data analysis/interpretation, all authors; manuscript drafting or manuscript revision for important intellectual content, all authors; approval of final version of submitted manuscript, all authors; agrees to ensure any questions related to the work are appropriately resolved, all authors; literature research, S.A.W., J.C., J.R.B., F.R., G.S., M.L., A.C.A., S.V.; clinical studies, S.A.W., J.C., K.O., J.R.B., M.A., M.L., A.C.A., S.V.; experimental studies, S.A.W., J.C., B.L., K.O., A.C., M.A., V.T., T.G., F.R., G.S., J.P.; statistical analysis, S.A.W., A.C.; and manuscript editing, S.A.W., J.C., K.O., J.R.B., A.C., F.R., G.S., J.P., M.L., A.C.A., S.V.

Disclosures of Conflicts of Interest: **S.A.W.** disclosed no relevant relationships. **J.C.** Activities related to the present article: disclosed no relevant relationships. Activities not related to the present article: is employed by and owns a part of InkSpace Imaging; the coil in this work was built using technology protected under U.S. patent 9,880,238. Other relationships: disclosed no relevant relationships. **B.L.** Activities related to the present article: disclosed no relevant relationships. Activities not related to the present article: is a board member, employee, and cofounder of InkSpace Imaging; holds stock in InkSpace Imaging; former institution (University of California, Berkeley) will receive royalties from InkSpace Imaging for patents on the printed MRI coils. Other relationships: disclosed no relevant relationships. **K.O.** disclosed no relevant relationships. **J.B.** disclosed no relevant relationships. **A.C.** Activities related to the present article: disclosed no relevant relationships. Activities not related to the present article: is a consultant for Subtle Medical; is a part-time employee of Skope MR; institution received grants from GE Healthcare and Philips; holds stock in LVIS, Subtle Medical, and Brain Key; is a scientific advisor for Brain Key. Other relationships: disclosed no relevant relationships. **M.A.** Activities related to the present article: disclosed no relevant relationships. Activities not related to the present article: holds stock in Arterys. Other relationships: disclosed no relevant relationships. **V.T.** Activities related to the present article: disclosed no relevant relationships. Activities not related to the present article: is employed by GE Healthcare. Other relationships: disclosed no relevant relationships. **T.G.** disclosed no relevant relationships. **F.R.** Activities related to the present article: disclosed no relevant relationships. Activities not related to the present article: is employed by GE Healthcare. Other relationships: disclosed no relevant relationships. **G.S.** disclosed no relevant relationships. **J.P.** disclosed no relevant relationships. **M.L.** Activities related to the present article: disclosed no relevant relationships. Activities not related to the present article: holds stock in InkSpace Imaging; institution licensed technology to InkSpace Imaging. Other relationships: disclosed no relevant relationships. **A.C.A.** Activities related to the present article: disclosed no relevant relationships. Activities not related to the present article: is a board member and consultant for InkSpace Imaging; institution holds U.S. patents 9,696,393 and 9,880,238. Other relationships: disclosed no relevant relationships. **S.V.** Activities related to the present article: disclosed no relevant relationships. Activities not related to the present article: holds stock in InkSpace Imaging. Other relationships: disclosed no relevant relationships.

References

1. Zhang T, Grafendorfer T, Cheng JY, et al. A semiflexible 64-channel receive-only phased array for pediatric body MRI at 3T. Magn Reson Med 2016;76(3):1015–1021.
2. Keil B, Alagappan V, Mareyam A, et al. Size-optimized 32-channel brain arrays for 3 T pediatric imaging. Magn Reson Med 2011;66(6):1777–1787.
3. Lopez Rios N, Foias A, Lodygensky G, Dehaes M, Cohen-Adad J. Size-adaptable 13-channel receive array for brain MRI in human neonates at 3 T. NMR Biomed 2018;31(8):e3944.
4. Corea JR, Flynn AM, Lechêne B, et al. Screen-printed flexible MRI receive coils. Nat Commun 2016;7(1):10839.
5. Corea JR, Lechene PB, Lustig M, Arias AC. Materials and methods for higher performance screen-printed flexible MRI receive coils. Magn Reson Med 2017;78(2):775–783.
6. Corea J, Lechene BP, Grafendorfer T, Robb F, Arias AC, Lustig M. Printed receive coil arrays with high SNR [abstr]. In: Proceedings of the Twenty-Fourth Meeting of the International Society for Magnetic Resonance in Medicine. Berkeley, Calif: International Society for Magnetic Resonance in Medicine, 2016; 2146.
7. Winkler SA, Corea J, Lechene B, et al. First clinical pilot study using screen-printed flexible MRI receive coils for pediatric applications [abstr]. In: Proceedings of the Twenty-Sixth Meeting of the International Society for Magnetic Resonance in Medicine. Berkeley, Calif: International Society for Magnetic Resonance in Medicine, 2018.
8. Roemer PB, Edelstein WA, Hayes CE, Souza SP, Mueller OM. The NMR phased array. Magn Reson Med 1990;16(2):192–225.
9. Edwards AD, Arthurs OJ. Paediatric MRI under sedation: is it necessary? what is the evidence for the alternatives? Pediatr Radiol 2011;41(11):1353–1364.
10. Sury MR, Smith JH. Deep sedation and minimal anesthesia. Paediatr Anaesth 2008;18(1):18–24.
11. Vasanawala SS, Lustig M. Advances in pediatric body MRI. Pediatr Radiol 2011;41(Suppl 2):549–554.
12. Keil B, Wald LL. Massively parallel MRI detector arrays. J Magn Reson 2013;229:75–89.
13. Keil B, Alagappan V, Mareyam A, et al. Size-optimized 32-channel brain arrays for 3T pediatric imaging. Magn Reson Med 2011;66(6):1777–1787.
14. Zhang T, Chowdhury S, Lustig M, et al. Clinical performance of contrast enhanced abdominal pediatric MRI with fast combined parallel imaging compressed sensing reconstruction. J Magn Reson Imaging 2014;40(1):13–25.
15. Mager D, Peter A, Tin LD, et al. An MRI receiver coil produced by inkjet printing directly on to a flexible substrate. IEEE Trans Med Imaging 2010;29(2):482–487.
16. Horch RA, Gore JC. 3D-printed RF coils for solution-state NMR: towards low-cost, high-throughput arrays [abstr]. In: Proceedings of the Twenty-Third Meeting of the International Society for Magnetic Resonance in Medicine. Berkeley, Calif: International Society for Magnetic Resonance in Medicine, 2015.
17. Uecker M, Lai P, Murphy MJ, et al. ESPIRiT: an eigenvalue approach to autocalibrating parallel MRI—where SENSE meets GRAPPA. Magn Reson Med 2014;71(3):990–1001.
18. Kellman P, McVeigh ER. Image reconstruction in SNR units: a general method for SNR measurement. Magn Reson Med 2005;54(6):1439–1447 [Published correction appears in Magn Reson Med 2007;58(1):211–212].